© 2019. Published by The Company of Biologists Ltd | Development (2019) 146, dev176701. doi:10.1242/dev.176701

RESEARCH ARTICLE

Loss of the E2 SUMO-conjugating enzyme *Ube2i* in oocytes during ovarian folliculogenesis causes infertility in mice

Amanda Rodriguez[1,2,*], Shawn M. Briley[1,3,*], Bethany K. Patton[1,2], Swamy K. Tripurani[1], Kimal Rajapakshe[4], Cristian Coarfa[4], Aleksander Rajkovic[5], Alexandra Andrieux[6], Anne Dejean[6] and Stephanie A. Pangas[1,2,3,4,‡]

ABSTRACT

The number and quality of oocytes within the ovarian reserve largely determines fertility and reproductive lifespan in mammals. An oocyte-specific transcription factor cascade controls oocyte development, and some of these transcription factors, such as newborn ovary homeobox gene (*NOBOX*), are candidate genes for primary ovarian insufficiency in women. Transcription factors are frequently modified by the post-translational modification SUMOylation, but it is not known whether SUMOylation is required for function of the oocyte-specific transcription factors or if SUMOylation is required in oocytes during their development within the ovarian follicle. To test this, the sole E2 SUMO-conjugating enzyme, *Ube2i*, was ablated in mouse oocytes beginning in primordial follicles. Loss of oocyte *Ube2i* resulted in female infertility with major defects in stability of the primordial follicle pool, ovarian folliculogenesis, ovulation and meiosis. Transcriptomic profiling of ovaries suggests that loss of oocyte *Ube2i* caused defects in both oocyte- and granulosa cell-expressed genes, including NOBOX and some of its known target genes. Together, these studies show that SUMOylation is required in the mammalian oocyte during folliculogenesis for both oocyte development and communication with ovarian somatic cells.

KEY WORDS: Reproduction, Fertility, Germ cell, Transcription factor, SUMOylation, PTM, NOBOX, UBE2I

INTRODUCTION

In mammals, oocyte development is an extended multi-stage process that begins in the embryo but is not completed until the oocyte is ovulated, resumes meiosis, and is fertilized in the adult. Postnatally, oocytes are enclosed by somatic cells and stored as a limited supply of non-growing primordial follicles, often referred to as the ovarian reserve. The number and quality of oocytes in primordial follicles are key determinants of the female reproductive lifespan, and reproduction continues until the supply of oocytes is exhausted. In women, primary ovarian insufficiency (POI) occurs when a woman loses normal ovarian function before the age of 40. This results in amenorrhea, elevated gonadotropins and estrogen deficiency. The underlying cause of POI is early oocyte depletion resulting in infertility (Pelosi et al., 2015), but in 90% of cases POI is idiopathic (Nelson, 2009). Previous studies have identified POI candidate genes, including oocyte-specific transcription factors such as newborn homeobox gene (*NOBOX*), spermatogenesis and oogenesis basic helix-loop-helix 1 (*SOHLH1*), and factor in the germline alpha (*FIGLA*), as well as the secreted factors growth and differentiation factor 9 (*GDF9*) and bone morphogenetic protein 15 (*BMP15*) (Bouilly et al., 2011; Bouilly et al., 2015; Jolly et al., 2019; Kumar et al., 2017; Qin et al., 2007; Suzumori et al., 2007; Zhao et al., 2007). Thus, POI may be driven by intra-oocyte defects as well as paracrine signaling defects between oocytes and their companion somatic cells.

SUMOylation is the covalent attachment of a small ubiquitin-like modifier (SUMO) protein to a lysine residue in a target protein. It is a highly dynamic and reversible post-translational protein modification and its substrates are often transcription factors (Rosonina et al., 2017). During folliculogenesis, an oocyte-specific gene expression program controls both oocyte development and communication with surrounding somatic cells; the transcription factor NOBOX plays a central role in oocyte development during folliculogenesis (Lechowska et al., 2011; Pangas et al., 2006; Rajkovic et al., 2004). *Nobox* expression begins at embryonic day (E) 15.5-17.5 in the mouse and continues to be expressed until the antral stage, when it is downregulated in developmentally competent oocytes (Belli et al., 2013). NOBOX in turn regulates expression of *Gdf9* and *Bmp15*, secreted members of the TGFβ family that promote granulosa and cumulus cell development. These genes moderate pathways for proliferation, cumulus expansion, and suppression of luteinization (Dong et al., 1996; Elvin et al., 1999; Su et al., 2004; Yan et al., 2001). Additional transcription factors necessary for oocyte development include SOHLH1, which controls expression of *Nobox* (Pangas et al., 2006), FIGLA, which controls expression of the zona pellucida genes (Liang et al., 1997; Soyal et al., 2000), and SOHLH2, which is required for early follicle formation (Ballow et al., 2006; Choi et al., 2008; Shin et al., 2017). Homozygous deletion of *Nobox*, *Sohlh1*, *Sohlh2*, *Figla* or *Gdf9* in mice all result in female sterility but do not grossly affect embryonic ovary development or significantly change oocyte numbers at birth (Choi et al., 2008; Dong et al., 1996; Pangas et al., 2006; Rajkovic et al., 2004; Soyal et al., 2000). However, defects in postnatal folliculogenesis are apparent in all of these mutants, with all but $Gdf9^{-/-}$ showing postnatal loss of oocytes prior to 21 days of age (Choi et al., 2008; Dong et al., 1996; Pangas et al., 2006; Rajkovic et al., 2004; Soyal et al., 2000).

Protein SUMOylation variably affects a number of functions, including altering subcellular localization, changing protein stability, and controlling transcriptional regulation (Geiss-Friedlander and Melchior, 2007; Hay, 2005). The covalent attachment of SUMO to substrate proteins occurs through an enzymatic cascade similar to that of ubiquitylation (Verger et al., 2003) and proteins can be mono- or poly-SUMOylated (Ulrich,

[1]Department of Pathology & Immunology, Baylor College of Medicine, Houston, TX 77030, USA. [2]Graduate Program in Molecular & Cellular Biology, Baylor College of Medicine, Houston, TX 77030, USA. [3]Graduate Program in Biochemistry & Molecular Biology, Baylor College of Medicine, Houston, TX 77030, USA. [4]Department of Molecular & Cellular Biology, Baylor College of Medicine, Houston, TX 77030, USA. [5]Department of Pathology, University of California, San Francisco, CA 94134, USA. [6]Nuclear Organization and Oncogenesis Unit, INSERM U993, Pasteur Institute, 75015 Paris, France.
*These authors contributed equally to this work

‡Author for correspondence (spangas@bcm.edu)

S.A.P., 0000-0001-5748-5844

Received 6 February 2019; Accepted 29 October 2019

Development (2019) 146, dev176701. doi:10.1242/dev.176701

2008). Central to the SUMOylation cascade is a single E2 SUMO-conjugating enzyme, UBE2I (ubiquitin-conjugating enzyme E2I; also known as UBC9), which is required for SUMOylation to occur. *Ube2i*$^{-/-}$ mice are embryonic lethal during early post-implantation prior to E7.5 as a result of mitotic defects in chromatin condensation, chromosome segregation and nuclear organization (Nacerddine et al., 2005).

In mammals, there are four SUMO proteins (SUMO1-4), and SUMO1, SUMO2 and SUMO3, as well as UBE2I, are known to be expressed in mouse oocytes (Ihara et al., 2008; Wang et al., 2010). *Ube2i* is expressed in mouse oocytes at least from postnatal day 13 (incompetent oocytes) to the germinal vesicle (GV) stage (fully grown oocyte), primarily in the nucleoplasm. *Ube2i* is downregulated following meiotic resumption (Ihara et al., 2008). Localization of SUMO1, SUMO2 and SUMO3 depends on the developmental stage of oocytes, with immature oocytes containing SUMO1 localized to the nuclear membrane and SUMO2/3 within the nucleoplasm; in meiotically competent oocytes, SUMO1 colocalizes with UBE2I-containing structures within the nucleoplasm that also contain SUMO2/3 (Ihara et al., 2008). Prior to the establishment of the ovarian reserve, SUMOylation is implicated in apoptotic pathways in response to DNA damage in mouse oocytes via ring finger protein 212 (RNF212), a SUMO E3 ligase (Qiao et al., 2018). In mouse oocytes, inhibition of *Ube2i* at the GV stage *in vitro* disrupts meiotic maturation and causes defects in spindle organization (Yuan et al., 2014). Overexpression of *Ube2i* by injection of *Ube2i* mRNA in meiotically incompetent oocytes stimulates transcription (Ihara et al., 2008). Other model organisms, including *Caenorhabditis elegans*, have provided additional insight into the roles of SUMOylation in oocytes. During meiotic progression in *C. elegans*, SUMOylation is responsible for regulating localization of various proteins, including BUB-1 (Pelisch et al., 2019). Chromosome congression in *C. elegans* is regulated by a SUMO-dependent protein network, supporting earlier work done in mouse oocytes (Pelisch et al., 2017; Yuan et al., 2014; Zhu et al., 2010). However, the role of *Ube2i* in developing mouse oocytes during ovarian folliculogenesis is currently unknown.

To determine the role of *Ube2i* in oocytes, an oocyte-specific conditional knockout (cKO) was created to delete a floxed *Ube2i* allele using *Gdf9-icre*, a well-characterized *cre* driver line for oocytes beginning at the primordial follicle stage, i.e. before oocyte growth and meiotic resumption (Lan et al., 2004). Analysis of female *Ube2i* cKO mice uncovered a complex infertility phenotype with defects appearing at multiple critical oocyte transition points, including stability of the ovarian reserve, communication with somatic cells, resumption of meiosis, and meiotic progression.

RESULTS

Oocyte-specific loss of *Ube2i* at the primordial follicle stage causes female infertility

To evaluate the role of SUMOylation in the developing postnatal ovary, male transgenic mice expressing a codon-improved Cre recombinase (iCre) driven by the mouse growth differentiation factor 9 (*Gdf9*) promoter (*Gdf9-iCre*) (Lan et al., 2004) were crossed to female *Ube2i*$^{loxP/loxP}$ mice (Fig. 1A) (Nacerddine et al., 2005). Genotypes were determined by PCR of genomic DNA (Fig. 1B) and loss of UBE2I was verified by immunofluorescence analysis (Fig. 1C). UBE2I localized to the oocyte nucleus in ovaries of 8-week-old *Ube2i*$^{loxP/loxP}$ control mice at the primordial, primary and secondary follicle stage (Fig. 1C), in addition to the nucleus of meiotically incompetent and GV-stage oocytes as previously described (Ihara et al., 2008). In contrast, UBE2I is predominantly cytoplasmic in the surrounding somatic granulosa cells (Fig. 1C). UBE2I was not detected in oocytes at any follicle stage in 8-week-old *Ube2i* cKO ovaries (Fig. 1C). Strong UBE2I-positive staining remained in *Ube2i* cKO in granulosa cells, as expected, demonstrating successful loss of *Ube2i* exclusively in oocytes of *Ube2i* cKO mice beginning at the primordial follicle stage.

To assess the effect of oocyte-specific loss of *Ube2i* on female fertility, sexually mature control and *Ube2i* cKO females were mated with wild-type males of proven fertility for 6 months (n=5 for each group). Although vaginal plugs were observed, *Ube2i* cKO females failed to produce offspring in contrast to control littermates, which exhibited normal numbers of pups per litter and litters per month (Fig. 2A). Gross anatomy of the female reproductive tracts of sexually immature mice (i.e. 3 weeks of age) suggested that the ovary was smaller in the *Ube2i* cKO compared with control (Fig. 2B), although the ovaries appeared morphologically normal with readily visible ovarian follicles on the surface (Fig. 2C). In support of these observations, wet weights of dissected ovaries from *Ube2i* cKO were significantly lower than that of controls at 4 weeks of age (P<0.01) (Fig. 2D).

Ube2i cKO mice show signs of ovarian failure due to loss of ovarian follicles in early adulthood

Because ovaries of 3-week-old *Ube2i* cKO females contained growing follicles (Fig. 2C), but mature female mice were infertile, *Ube2i* cKO female mice were tested for their ability to ovulate using exogenous gonadotropin stimulation and oocyte collection from the oviduct ampulla. Eighteen hours after hormone injection, the majority of *Ube2i* cKO females failed to ovulate (6/10) with the remainder (4/10) ovulating significantly fewer oocytes than controls (Fig. 3A). At the time of collection, control oocytes had reached meiotic metaphase II (MII); in contrast, *Ube2i* cKO mutant oocytes appeared to have resumed meiosis and undergone germinal vesicle breakdown (GVBD), but none showed a polar body, suggesting the mutant oocytes had not completed MI (data not shown). Therefore, to test the ability of *Ube2i* cKO oocytes to resume meiosis, GV oocytes were collected from equine chorionic gonadotropin (eCG)-stimulated mice for *in vitro* maturation and monitored for 24 h with live imaging. During this time frame, 91.4% of control oocytes underwent GVBD and 78.1% proceeded to extrude a polar body (Fig. 3B; n=35). In contrast, significantly fewer GV oocytes (53.8%) from *Ube2i* cKO mice underwent GVBD (P<0.01, Fisher's exact test), and all failed to extrude polar bodies (P<0.001, Fisher's exact test) (Fig. 3B; n=11). Because *in vitro*-matured oocytes from *Ube2i* cKO mice did not extrude polar bodies, spindle morphology and chromosome alignment were analyzed in oocytes collected from superovulated mice following eCG and human chorionic gonadotropin (hCG) stimulation. Immunofluorescence staining of α-tubulin did not identify any spindle abnormalities in *Ube2i* cKO mice compared with the control mice, and chromosome alignment also appeared grossly normal (Fig. 3C).

Ovaries from mice aged 2 weeks to 6 months were examined by histology and follicles were quantified to determine if there were defects in the ovarian reserve or in folliculogenesis (Fig. 4). Ovaries from sexually immature 2-week-old and 3-week-old mutant mice did not reveal any gross changes in histology or morphometric follicle count differences between genotypes (Fig. 4A-C, Fig. S1A, B). In sexually mature 8-week-old mice, compared with control (Fig. 4D), *Ube2i* cKO ovaries lacked later-stage follicles, with significantly reduced numbers of preantral and antral follicles in addition to a complete lack of corpora lutea (Fig. 4E,F, Fig. S1C). At 12-14 weeks of age, the lack of folliculogenesis in the *Ube2i* cKO was obvious by histology (Fig. 4H,I), with significantly reduced

Development (2019) 146, dev176701. doi:10.1242/dev.176701

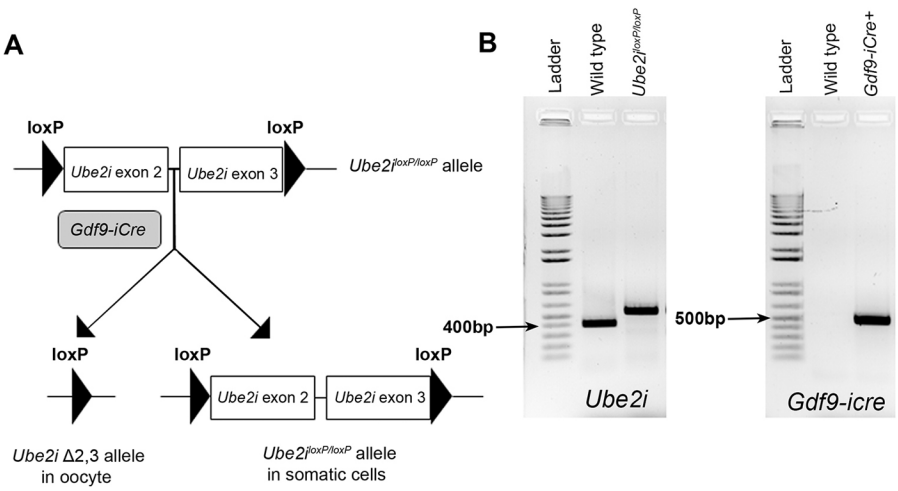

Fig. 1. *Gdf9-iCre* was used to delete *Ube2i*$^{loxP/loxP}$ in oocytes of primordial follicles. (A) *loxP* sites flank exons 2 and 3 of *Ube2i* enabling oocyte-specific deletion of *Ube2i* in primordial follicles when crossed to *Gdf9-iCre*. (B) PCR genotyping results for *Ube2i* in genomic DNA from wild-type and *Ube2i*$^{loxP/loxP}$*Gdf9-icre*+ mice for *Ube2i*$^{loxP/loxP}$ (left) and *Gdf9-icre* (right). Expected sizes of PCR products are shown for the wild-type and floxed alleles as well as cre. (C) Immunofluorescence for UBE2I (green) in control mice shows nuclear localization in the oocyte (Oo) in primordial (PrF), primary (PF) and secondary (SF) follicles with cytoplasmic localization in the surrounding somatic granulosa cells (GC). There is a loss of UBE2i immunoreactivity in *Ube2i* cKO oocytes of all stages with retained expression (green) in granulosa cells. Blue, DAPI. Scale bars: 25 µm.

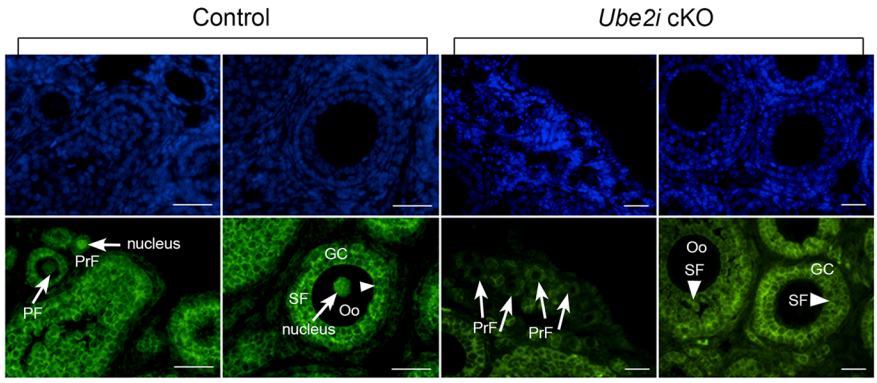

numbers of primordial, secondary and antral follicles, no corpora lutea, along with an increased number of atretic follicles (Fig. S1D). By 6 months of age, there was complete follicle depletion in *Ube2i* cKO ovaries whereas control ovaries exhibited ongoing folliculogenesis and corpora lutea (Fig. 4J-L). As ovaries of *Ube2i* cKO females showed premature loss of ovarian follicles, key serum markers of primary ovarian failure were tested in young adult (8-week-old) mice, including follicle stimulating hormone (FSH) and anti-Müllerian hormone (AMH). FSH and AMH were chosen as they are established clinical markers of ovarian function (Sun

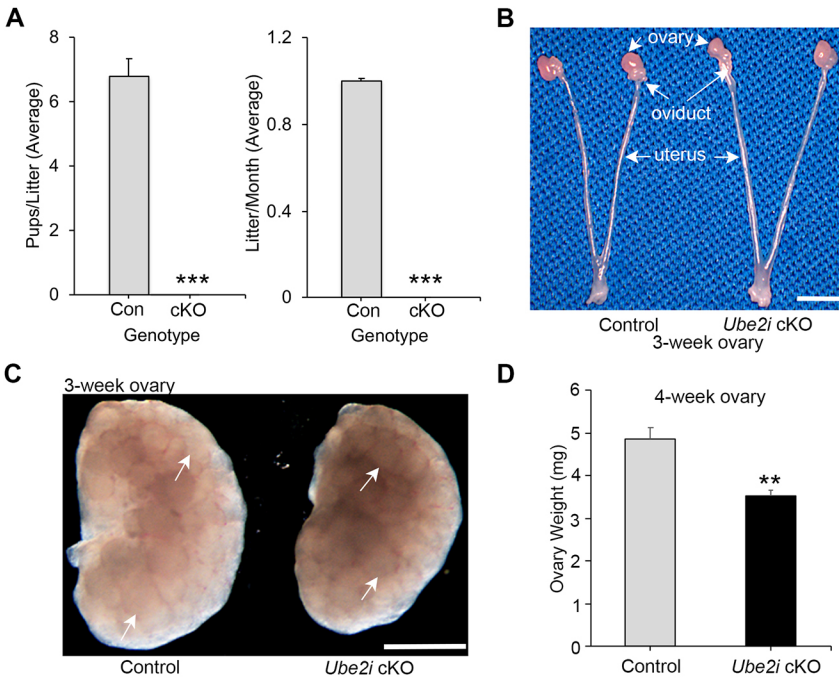

Fig. 2. *Ube2i* cKO female mice are infertile. (A) Fertility data of control (Con) and *Ube2i* cKO (n=5 breeding pairs per genotype) bred in continuous paired matings for 6 months. Average pups per litter (left) and litters per month (right) are shown as mean+s.e.m. ***P<0.001 by Student's t-test. (B) Gross dissection of representative control and *Ube2i* cKO reproductive tracts from 3-week-old mice show no overall morphological differences. Ovary, oviduct and uterus are indicated in both genotypes. Scale bar: 5 mm. (C) Image of dissected ovaries (shown in B) at higher magnification, showing the smaller size of *Ube2i* cKO ovary compared with control, with visible ovarian follicles seen in both (arrows). Scale bar: 1 mm. (D) Quantification of average weight of both ovaries from 4-week-old control (n=4 mice) and *Ube2i* cKO (n=3 mice) females. Mean+s.e.m. is shown. **P<0.01 by Student's t-test.

Development (2019) 146, dev176701. doi:10.1242/dev.176701

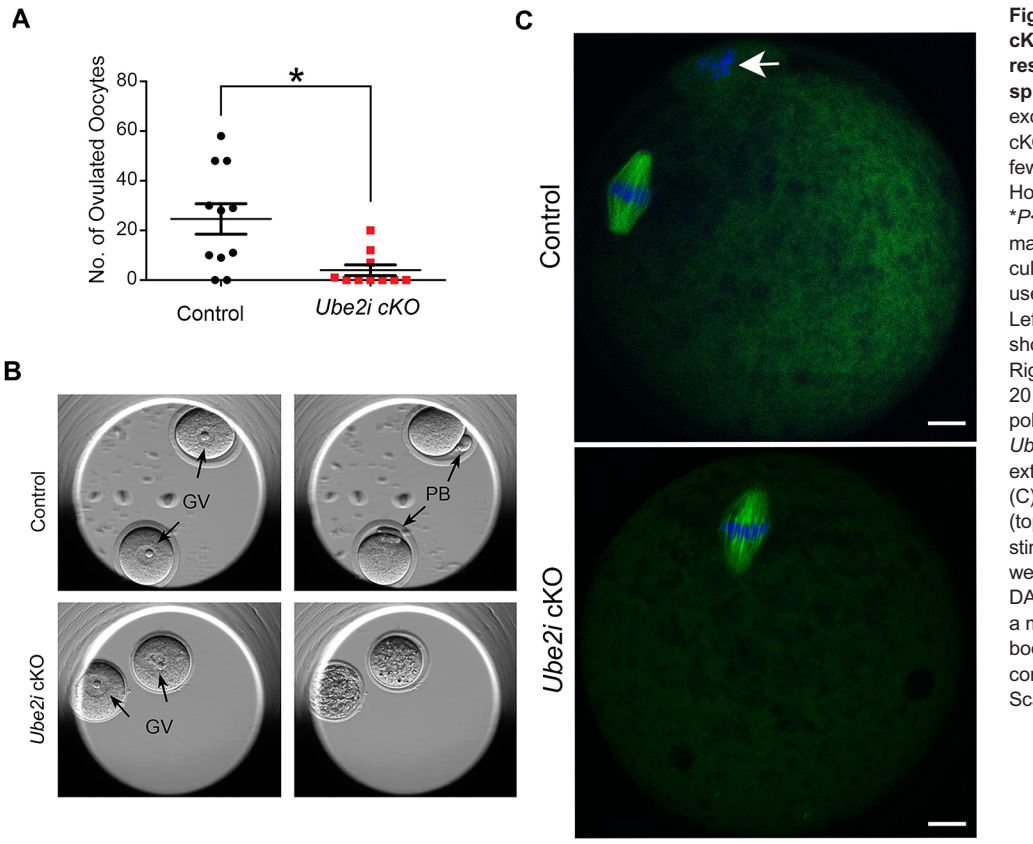

Fig. 3. Oocytes collected from *Ube2i* cKO females have defects in meiotic resumption and progression but normal spindle morphology. (A) Following exogenous gonadotropin treatment, *Ube2i* cKO females (n=10) ovulate significantly fewer oocytes than do controls (n=11). Horizontal bars shows average and s.e.m. *P<0.05 by Student's t-test. (B) Oocytes matured *in vitro* using the Embryoscope culture system (two oocytes per well) were used for measuring meiotic resumption. Left: oocytes prior to *in vitro* maturation showing GV stage in both genotypes. Right: control and *Ube2i* cKO oocytes after 20 h of culture. Control oocytes extrude polar bodies (PB) and reach MII, whereas *Ube2i* oocytes undergo GVBD, but fail to extrude polar bodies and are degenerating. (C) Ovulated oocytes collected from control (top) and *Ube2i* cKO (bottom) mice stimulated with eCG and hCG. Oocytes were stained for α-tubulin (green) and DAPI (blue). Top: a control egg containing a metaphase II spindle and extruded polar body (arrow). Bottom: a *Ube2i* cKO oocyte containing an intact metaphase I spindle. Scale bars: 10 µm.

et al., 2008; Visser et al., 2012). Both hormones were significantly altered in *Ube2i* cKO female mice. FSH, a pituitary hormone that is upregulated when there is loss of ovarian negative feedback, was significantly increased in *Ube2i* cKO compared with controls (P<0.001) (Fig. S2A). AMH, an ovarian marker used to test levels of the ovarian reserve, was significantly downregulated (Fig. S2B).

Ube2i cKO ovaries show abnormal expression of genes involved in development, morphogenesis, and signal transduction

To understand how loss of oocyte UBE2I affects gene expression, RNA sequencing (RNA-seq) was performed on triplicate samples of whole ovaries from 2-week-old control and *Ube2i* cKO ovaries. This time point was chosen because there were no overt histological defects (Fig. 4A-C) or changes to follicle numbers (Fig. S1A); thus, differences due to structural changes to the ovary should be largely avoided. Whole ovaries were chosen so that expression differences for both oocytes and somatic cells could be queried. In total, 585 significant differentially expressed genes (DEGs) were identified, including 208 that were upregulated and 377 that were downregulated in *Ube2i* cKO ovaries using the parameters of P<0.05 and fold change>1.5 (up or down) (Fig. 5A,B, Table S1A). The DEG list is presented in Table S1A. Significantly downregulated genes included known oocyte-expressed factors, such as bone morphogenetic protein 15 (*Bmp15*), ret finger protein-like 4 (*Rfpl4*), spalt-like transcription factor 4 (*Sall4*) and SMAD family member 6 (*Smad6*). Significantly upregulated genes included the oocyte-expressed synaptonemal complex protein 3 (*Sycp3*), and genes not normally highly expressed in the ovary, such as natriuretic peptide receptor 1 (*Npr1*) and kelch-like family member 1 (*Klhl1*).

To investigate biological functions, gene ontology (GO) analysis was performed for all DEGs (Fig. 5C), as well as subsets that were upregulated or downregulated (Table S1B). Analyzing all DEGs, there was statistical enrichment in biological processes involved in development, morphogenesis, signal transduction, and apoptosis (Fig. 5C). There were fewer significant GO terms for the group of upregulated genes in the *Ube2i* cKO, which included negative regulators of cell differentiation and negative regulators of transcription (Table S1B). In contrast, DEGs that were downregulated belong to GO categories for development, negative regulation of the BMP pathway, and signal transduction (Table S1B). The GO category, 'Multicellular Organism Development' was further analyzed (Table S1C) for gene function. The largest category of DEGs was transcription factors (7/21), two of which were known to be SUMOylated (*Eya4*, *Hoxa13*). Other categories of DEGs included RNA-binding proteins and factors necessary for signal transduction (Table S1C).

Ingenuity pathway analysis (IPA) software was then used to identify top upstream regulators that contribute to the observed gene expression alterations in *Ube2i* cKO mice (Fig. 5D, Table S2A). Statistically significant upstream regulators included PR/SET Domain 1 (PRDM1) and nuclear receptor interacting protein 1 (NRIP1). As SUMOylation disproportionately affects transcription factor function (Rosonina et al., 2017), IPA was used to filter for upstream transcriptional regulators (Table S2). Eighty-six transcriptional regulators were identified. This list included key oocyte transcription factors, such as NOBOX, and granulosa cell transcription factors, such as GATA4 and ID1 (Fig. 5E, Table S2A). Filtering the data set by 'growth regulatory pathways' indicated that regulators of the DEGs included BMP15 and AMH (Fig. 5D, Table S2B), two key oocyte and granulosa cell pathways.

Key oocyte genes were selected and transcripts quantified in 3-week-old control and *Ube2i* cKO ovaries (Fig. 6A). This included *Nobox* and the NOBOX target genes *Gdf9* and *Bmp15*. Surprisingly, whereas *Nobox* mRNA levels were significantly increased in ovaries from the *Ube2i* cKO, *Bmp15* and *Gdf9* expression were significantly

Development (2019) 146, dev176701. doi:10.1242/dev.176701

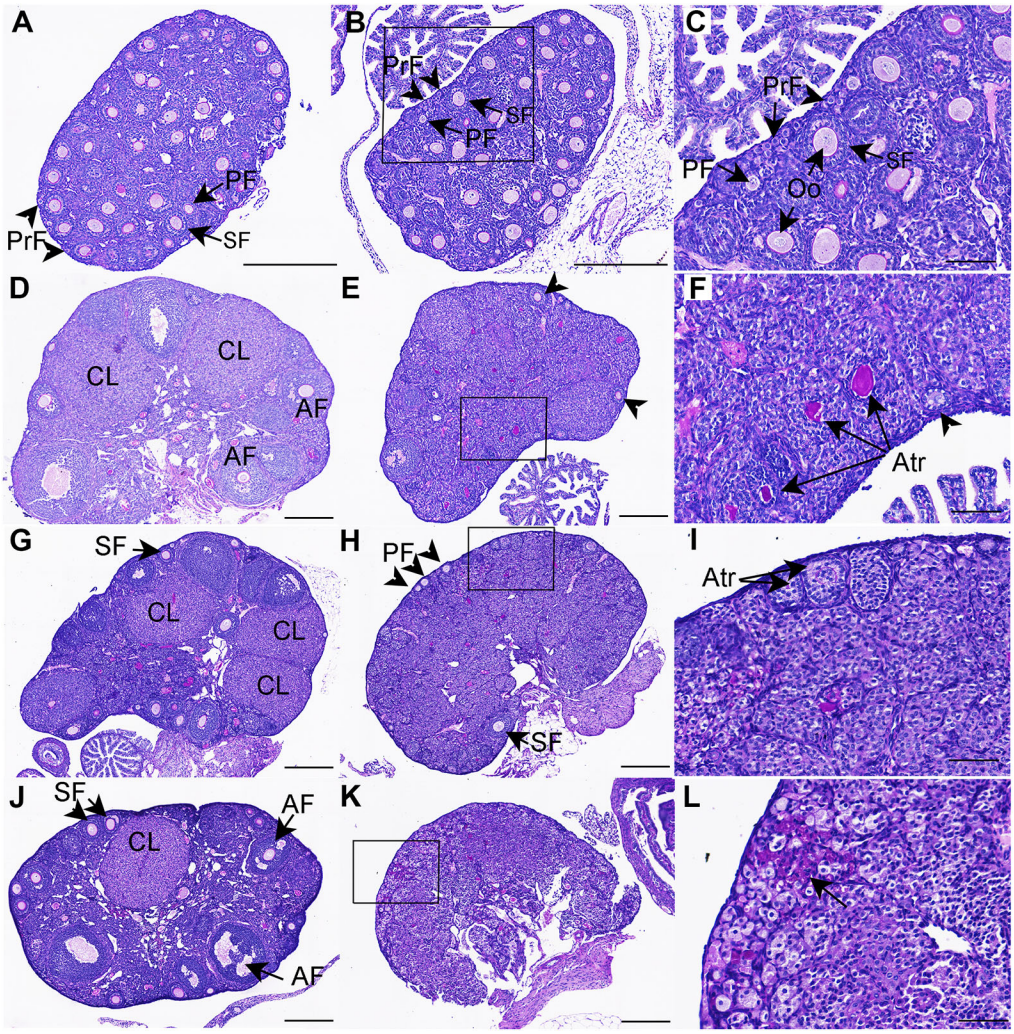

Fig. 4. Ovarian follicle development is impaired in mice with oocytes lacking *Ube2i*. (A-L) Histological sections of control (A,D,G,J) and *Ube2i* cKO (B,C,E,F,H,I,K,L) ovaries were stained with periodic acid-Schiff and compared at multiple ages. (A) A 2-week-old control ovary showing primordial (PrF), primary (PF) and secondary (SF) follicle stages. (B,C) A 2-week-old *Ube2i* cKO ovary showing similar stages as the control ovary and follicles that contain growing oocytes (Oo). C shows a higher magnification of the boxed area in B. (D) A control ovary at 8 weeks of age showing development of corpora lutea (CL) and antral follicles (AF). (E,F) The *Ube2i* cKO ovary only shows smaller follicles (arrowheads) and atretic follicles (Atr). F shows a higher magnification of the boxed area in E. (G) A 14-week-old control ovary showing developing follicles of all stages, including CL. (H,I) An ovary section of a 14-week-old *Ube2i* cKO showing few follicles at primary (PF) and secondary (SF) stages and some atretic follicles (Atr) but no large follicles or CL. I shows a higher magnification of the boxed area in H. (J) A 6-month-old control ovary showing all follicle stages and CL. (K,L) A 6-month-old *Ube2i* cKO ovary showing atrophy and no follicles. L shows a higher magnification of the boxed area in K. Arrow in L indicates periodic acid-Schiff-positive material typical of inflammatory infiltrate found in aged ovaries (Briley et al., 2016). Scale bars: 200 µm (A,B,D,E,G,H,J,K); 40 µm (C,F,I,L).

decreased, suggesting defects in NOBOX regulation of its target genes (Fig. 6A). Therefore, NOBOX protein was analyzed to verify whether loss of SUMOylation affected NOBOX protein stability or its cellular localization, either of which could cause a loss in target gene transcription. Mouse NOBOX is known to contain a nuclear localization site and is constitutively nuclear throughout folliculogenesis prior to being downregulated in oocytes of antral follicles (Belli et al., 2013; Rajkovic et al., 2004; Suzumori et al., 2002). No difference in NOBOX nuclear localization was found between control and *Ube2i* cKO oocytes at any follicle stage at 2 weeks and 3 weeks of age (Fig. S3A-E). In addition, NOBOX was degraded similarly in oocytes of antral follicles in both control and *Ube2i* cKO mice (Fig. S3F,E). Furthermore, immunoblotting for NOBOX in 2-week-old ovaries showed similar levels of protein in the control versus the mutant (Fig. S3H).

Because NOBOX localization and quantity did not change, defects in NOBOX target gene expression could result from indirect disruption of NOBOX signaling (e.g. loss of a NOBOX co-regulator) or, alternatively, direct disruption (e.g. loss of NOBOX SUMOylation). It is not known whether NOBOX is post-transcriptionally modified. Prediction software (GPS-SUMO) (Zhao et al., 2014) indicated that mouse NOBOX contains one consensus SUMOylation site at amino acid position 125 and one non-consensus site at amino acid 97. As SUMOylation is a dynamic process involving conjugation and deconjugation of SUMO, often only a fraction (often less than 1%) of a protein is SUMOylated at a given time (Johnson, 2004). In addition, SUMO can be conjugated singly or in chains (Békés et al., 2011). Therefore, to determine whether NOBOX can be SUMOylated, HEK-293T cells were transiently co-transfected with a FLAG-tagged mouse NOBOX overexpression vector along with non-deconjugatable forms of SUMO1 or SUMO2/3 that were Myc-tagged (indicated as Myc-SUMO1ρ or Myc-SUMO2/3ρ) (Rohira et al., 2013). Cell extracts were immunoprecipitated with anti-FLAG antibodies and immunoblotted for Myc. As expected, no NOBOX SUMOylation was detected when cells were untransfected, or if Myc-SUMO1ρ or Myc-SUMO2/3ρ were not co-expressed (Fig. 6B). Immunoprecipitation (anti-FLAG) of FLAG-NOBOX followed by immunoblotting (anti-Myc) for the SUMO proteins identified bands of the appropriate molecular weight that likely correspond to mono- and poly-SUMOylated NOBOX (Fig. 6B). These data indicate that NOBOX contains functional SUMOylation sites and can be SUMOylated by either SUMO1 or SUMO2/3 *in vitro*.

DISCUSSION

There is limited information regarding the role of UBE2I-mediated SUMOylation in postnatal oocyte development, particularly during ovarian follicle development. Previous studies have focused on the role of SUMOylation in oocytes during meiotic resumption, as GV oocytes are readily obtained and manipulated using microinjection of antibodies, RNA, siRNA, or with pharmacological intervention.

Development (2019) 146, dev176701. doi:10.1242/dev.176701

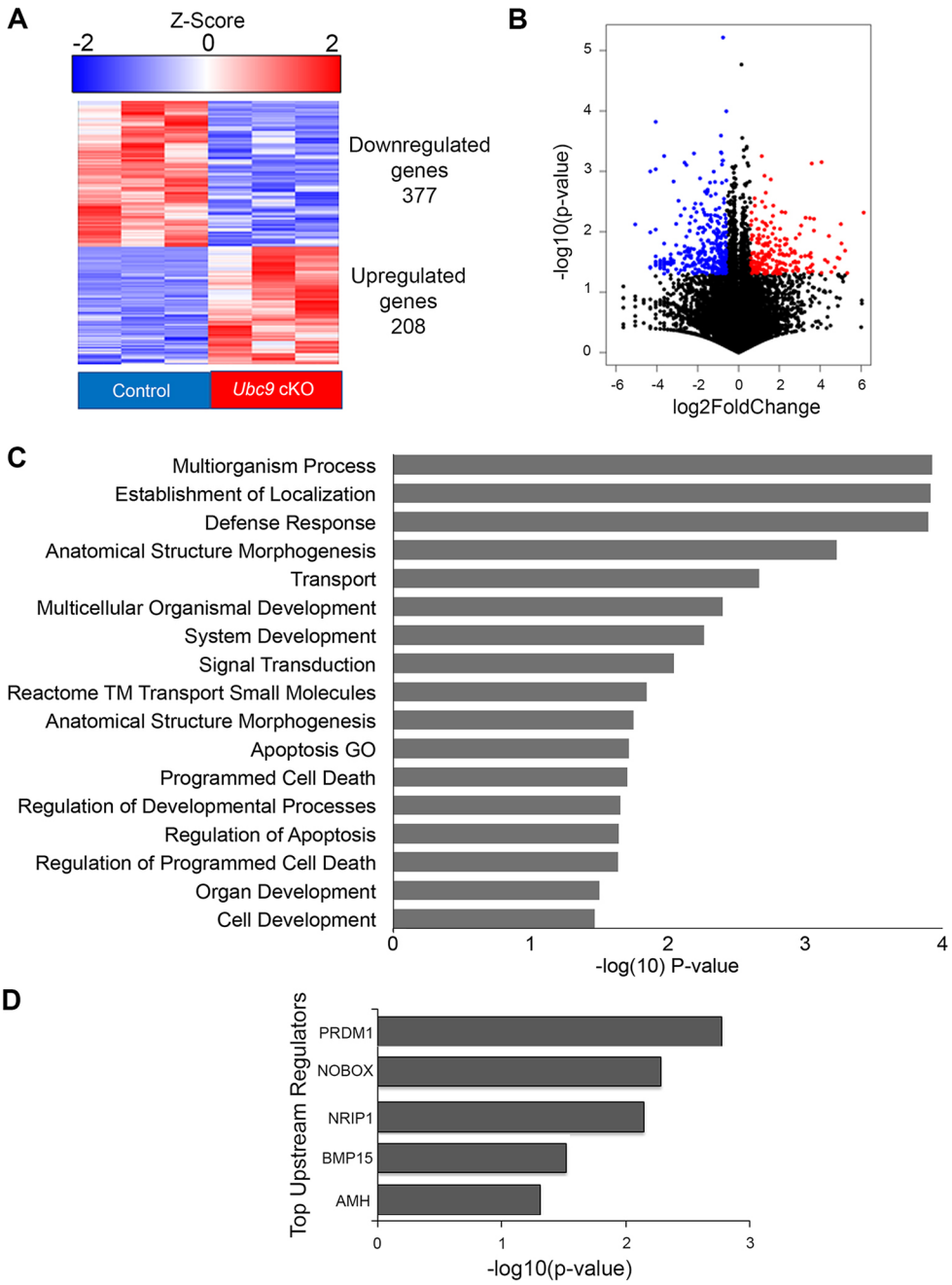

Fig. 5. Loss of *Ube2i* in the oocyte alters the ovarian transcriptome.
(A) Hierarchical clustering of significantly different genes in an RNA-seq analysis of 2-week-old *Ube2i* cKO ovaries compared with control ovaries (P<0.05 and fold change ±1.5). Three independent pools of three ovaries per genotype were analyzed. Downregulated genes are shown in blue and upregulated genes are indicated in red. (B) Volcano plot displaying DEGs identified in *Ube2i* cKO mice. The *y*-axis corresponds to $\log_{10}$ (*P*-value) and the *x*-axis displays the $\log_2$ fold change value. The blue dots represent significantly decreased transcripts; the red dots represent the transcripts for which expression levels were significantly increased. (C) GO analysis of DEGs ordered by –log(10) *P*-value. (D) Top 5 enriched upstream regulators identified from IPA of the *Ube2i* cKO transcriptome. *x*-axis represents the –log of the *P*-value.

These *in vitro* studies highlight a requirement for SUMOylation in meiotic resumption, meiotic progression and spindle formation during oocyte maturation (Feitosa and Morris, 2018; Yuan et al., 2014), as well as transcription (Ihara et al., 2008). However, no *in vivo* models testing SUMOylation in developing oocytes have been published to date. The present study extends the known developmental time frame during which SUMOylation is required in oocytes by demonstrating that oocyte-expressed *Ube2i* is required for female fertility in mice during follicle development from the primordial stage onward. As expected with loss of a major post-translational modification cascade during an expended developmental period, there are multiple facets to the phenotype of *Ube2i* cKO mice, including premature loss of ovarian follicles, impaired oocyte development during folliculogenesis, and altered meiotic maturation and progression. Meiosis and oocyte growth are processes that can be uncoupled (Dokshin et al., 2013), and SUMOylation appears to play crucial roles in both of these pathways during oogenesis.

During folliculogenesis, oocytes remain arrested in the diplotene phase of prophase I of meiosis, but once recruited into the growing follicle pool, transcribe and store RNA necessary for both follicle development and early embryo development. *Gdf9-icre* is a well-characterized cre recombinase driver for oocytes beginning at the primordial follicle stage around postnatal day 3 in mice (Lan et al., 2004) and loss of UBE2I in *Ube2i* cKO oocytes in primordial follicles was verified. Although adult *Ube2i* cKO female mice are infertile, the first wave of folliculogenesis appears to be largely unaffected as there were no overt histologic defects and all stages of preantral follicle development could be seen prior to 3 weeks of age. However, folliculogenesis is abnormal, as indicated by the lack of oocytes retrieved from approximately half of hormone-stimulated immature mice. Furthermore, for those *Ube2i* cKO mice from which

Development (2019) 146, dev176701. doi:10.1242/dev.176701

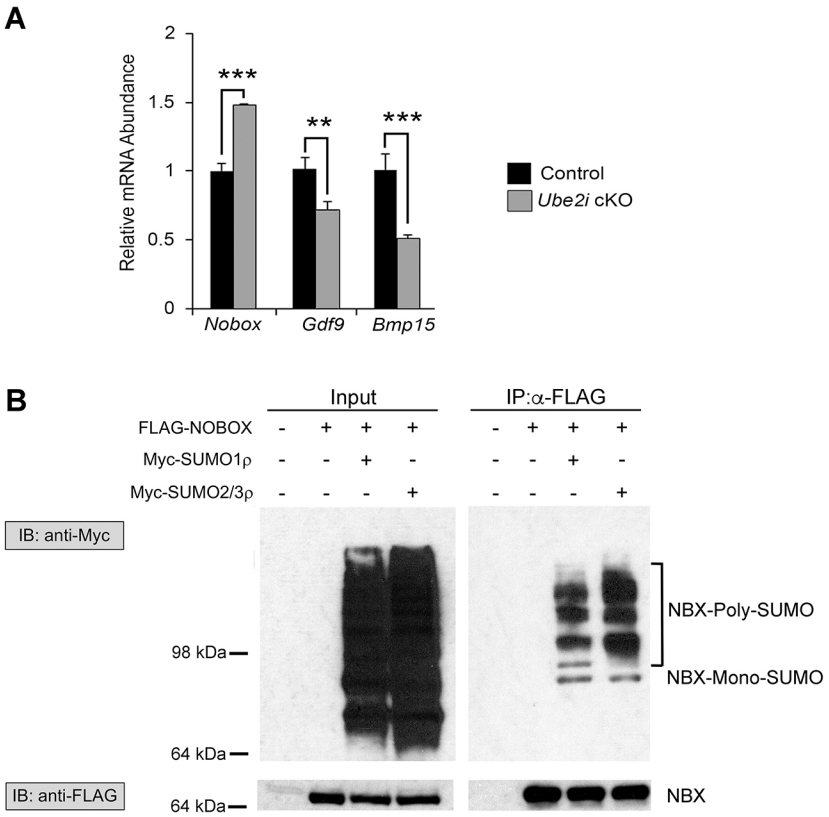

Fig. 6. Loss of oocyte SUMOylation in *Ube2i* cKO mice alters the expression of NOBOX and its downstream targets and NOBOX is SUMOylated *in vitro*. (A) qPCR analysis of mRNA from adult control and *Ube2i* cKO ovaries for *Nobox* and the NOBOX target genes *Gdf9* and *Bmp15*. Ovaries were collected from >3 mice per genotype per gene. Mean+s.e.m. are shown. Significant changes were seen in the relative quantity of *Nobox*, *Gdf9* and *Bmp15*. Control values were set to equal 1 and data were normalized to *Gapdh*. ***P*<0.01; ****P*<0.001. (B) HEK-293T cells were transfected with no plasmid, FLAG-NOBOX alone, or FLAG-NOBOX with Myc-SUMO1ρ or Myc-SUMO2/3ρ. Immunoprecipitation (IP) of cell lysates was performed using M2-FLAG beads to pull down NOBOX (NBX). Immunoblots for Myc (top blots) show Myc-SUMO in input and distinct bands in the IP eluent likely corresponding to mono- and poly-SUMOylated NOBOX. Control immunoblots for FLAG expression (bottom) show FLAG-NOBOX visible in the input samples and that it was successfully immunoprecipitated. IP-IB experiments were repeated in triplicate independent experiments.

oocytes could be collected, the oocytes had major defects in meiotic progression. Approximately half of *in vitro*-matured oocytes could not resume meiosis (i.e. remained at the GV stage), whereas other oocytes arrested in MI following GVBD but before polar body extrusion (PBE). A previous study has shown that knockdown (KD) *in vitro* of *Ube2i* or *Sumo1* in isolated GV-stage oocytes using siRNA microinjection reduces GVBD by approximately 50% of control values (Yuan et al., 2014), which is similar to the decreased percentage of mutant oocytes undergoing GVBD in our present study. However, in contrast to our study, approximately 40% of *Ube2i* KD oocytes retain the ability to undergo PBE compared with their controls (Yuan et al., 2014), whereas none of the *Ube2i* cKO oocytes are able to proceed to PBE. There are several potential explanations for this, including a difference in methodologies (i.e. a KD may be less efficient than the cKO or UBE2I protein may be more stable). It is also possible that the difference between the *Ube2i* KD and the *Ube2i* cKO represent acute versus developmental differences that require SUMOylation. For example, in studies that utilize fully grown GV oocytes, oocytes are transcriptionally quiescent and thus the RNA/protein needed for PBE may already be present, such that a KD of *Ube2i* will have reduced effect. In contrast, with the *Ube2i* cKO, loss of SUMOylation may disrupt the function of a transcription factor that is required to regulate expression of a key gene needed for PBE but is stored prior to the GV stage. Indeed, a large of number transcription factors with uncharacterized ovarian functions were found to be downregulated in *Ube2i* cKO ovaries. Furthermore, additional transcription factors that may be normally expressed in the cKO could be functionally regulated by SUMOylation and, thus, a biochemical or proteomic analysis will be required to detect these changes. Additional RNA profiling of GV control and *Ube2i* cKO oocytes at different stages would identify missing or novel components expressed prior to the GV stage during follicle development that are required for the MI-to-MII transition.

Understanding the MI block in *Ube2i* cKO requires additional study but does not appear to relate to chromosome alignment or spindle assembly, as these appear normal. This is in direct contrast to *in vitro Ube2i* KD studies that identified abnormal spindle assembly and chromosome alignment. The meiotic arrest in *Ube2i* cKO is also earlier than that seen in recent studies showing SUMOylation is required to maintain sister cohesion in late anaphase and telophase, as loss of PIAS1, a SUMO E3 ligase, activity allows progression to anaphase/telophase but also causes premature separation of sister chromatids (Ding et al., 2018). Thus, there are likely to be additional uncharacterized roles of SUMOylation during the MI-to-MII transition that will require further study.

Defects in ovulation and meiotic maturation are likely major contributors to infertility in *Ube2i* cKO young mice, and complete loss of oocytes within follicles is an additional contributing factor in adulthood. Ovarian function can be monitored by serum markers, FSH and AMH. The pituitary gonadotropin, FSH, is pathologically increased in *Ube2i* cKO females in young adulthood (e.g. 2 months of age), in line with the altered folliculogenesis (i.e. loss of preantral and antral stage follicles). Serum AMH has gained acceptance as a marker of the ovarian reserve (Dewailly et al., 2014; Oh et al., 2019; van Houten et al., 2010). AMH is produced from granulosa cells of small growing follicles and is indirectly correlated with the primordial follicle pool (Kevenaar et al., 2006). In *Ube2i* cKO mice, a significant reduction in serum AMH is detected at 8 weeks of age, and is likely the result of the decreased preantral follicles, which produce the highest levels of AMH (Munsterberg and Lovell-Badge, 1991; Salmon et al., 2004). Although AMH has been characterized as a negative regulator of the primordial follicle pool, the dynamics of primordial follicle recruitment did not appear to be altered in the *Ube2i* cKO and no evidence of global activation of the primordial follicle pool was seen at any age examined. In contrast, there is progressive loss of ovarian follicles, starting with more

Development (2019) 146, dev176701. doi:10.1242/dev.176701

advanced follicle stages (i.e. corpora lutea and antral follicles) followed by secondary and primordial follicles by 3-4 months of age. By 6 months of age, all follicles had been depleted in the *Ube2i* cKO. It is currently unclear if the loss of primordial follicles is due to loss of SUMOylation directly in primordial follicle oocytes or whether the stability of the pool is indirectly affected by changes to intraovarian signaling. Additional models using stage-specific cre recombinase models will be required to test these questions.

The RNA-seq analysis of 2-week-old ovaries identified a number of changes to both oocyte and somatic cell genes. Many of these changes are developmental and include an upregulation of negative regulators of cell differentiation and transcription and a downregulation of genes involved in regulation of ovarian follicle development, multicellular organism development, signal transduction and intracellular signaling. Both *Gdf9* and *Bmp15* were downregulated in *Ube2i* cKO ovaries. In addition, the IPA analysis showed that genes related to the BMP15 signaling pathway were significantly disrupted. BMP15, an oocyte-specific member of the TGFβ family, along with GDF9, forms key homo- and heterodimers that are crucial for folliculogenesis (Peng et al., 2013; Su et al., 2008; Su et al., 2004; Yan et al., 2001). Mice double mutant for *Gdf9* and *Bmp15* ($Gdf9^{+/-}Bmp15^{-/-}$) have aberrant meiotic resumption and decreased ovulation (Su et al., 2004; Yan et al., 2001). It is likely that disruption of the bi-directional oocyte-granulosa cell regulatory loop in *Ube2i* cKO is mediated, at least in part, by the changing levels of these two key oocyte-secreted mediators of somatic cell function, leading to defects in folliculogenesis and ovulation.

Finally, SUMOylation appears to be important for the function of the oocyte-specific transcription factor cascade that facilitates oogenesis, including NOBOX, which regulates expression of *Gdf9* and *Bmp15*. How SUMOylation affects the function of transcription factors is protein specific, and includes alterations in protein localization, activity and stability (Hilgarth et al., 2004). In the *Ube2i* cKO, *Nobox* transcript was upregulated but NOBOX target genes were downregulated. *Nobox* is known to be upregulated at least in part by SOHLH1 (Pangas et al., 2006), indicating that loss of the SUMOylation cascade affects the ability of SOHLH1 to appropriately regulate one or more of its target genes, either directly or indirectly. Post-translational modifications of NOBOX have not been characterized, but our data show that NOBOX contains predicted consensus and non-consensus SUMOylation sites, and the ability to be SUMOylated *in vitro* with either SUMO1 or SUMO2/3. In the *Ube2i* cKO, NOBOX localizes to the oocyte nucleus irrespective of UBE2I activity, and, although the transcript is increased, there is no effect on protein stability as ovaries contain similar levels of NOBOX. Because NOBOX was identified in the informatics analysis of the transcriptomic changes as a key upstream regulator, it is likely that SUMOylation regulates either NOBOX transcriptional activity or possibly interaction with co-factors. Clearly, some NOBOX target genes are more sensitive to loss of SUMOylation, including *Bmp15* and *Gdf9*. It is currently unclear whether NOBOX has differential target genes when it is SUMOylated, which will require further study. Transcription factors such as NOBOX are produced in oocytes throughout folliculogenesis (Rajkovic et al., 2004), but it is not known whether they regulate the same genes at different stages or if they have stage-specific targets. Post-translational modifications such as SUMOylation may be the mechanism for changing transcription factor target selection in the oocyte during different stages of follicle development. In addition to uncovering a role for SUMOylation in an oocyte-specific transcription factor, this study provides new evidence that SUMO conjugation modulates key transition stages that regulate female fertility, including primordial follicle stability, folliculogenesis and meiotic competence. Characterizing the 'SUMO-ome' (Nie et al., 2009) of oocytes could unlock novel regulatory circuits during oocyte development.

MATERIALS AND METHODS

Experimental mice

All experimental procedures were performed in compliance with the National Institutes of Health Guide for the Care and Use of Laboratory Animals, and Institutional Animal Care and Use Committee-approved animal protocols at Baylor College of Medicine. The *Ube2i* floxed allele was previously generated by inserting *loxP* sites flanking exons 2 and 3 (Nacerddine et al., 2005). $Ube2i^{loxP/+}$ mice were crossed to generate $Ube2i^{loxP/loxP}$ females, which were mated with *Gdf9iCre+* males. $Ube2i^{loxP/+}$ *Gdf9-iCre+* males were crossed to $Ube2i^{loxP/loxP}$ females to generate $Ube2i^{loxP/loxP}$ *Gdf9-iCre+*. The generation and genotyping of *Gdf9-iCre* mice has been described elsewhere (Lan et al., 2004). PCR analysis of genomic DNA from tail (<21 day) or ear punches was used for genotyping as described (Nacerddine et al., 2005). Littermates that were negative for *cre* were used as controls in all experiments to reduce potential differences in genetic backgrounds. Experimental mice were maintained on a hybrid C57BL/6J/129S7/SvEvBrd genetic background. For ease of reading, $Ube2i^{loxP/loxP}$ are referred to as 'controls' and $Ube2i^{loxP/loxP}$ *Gdf9-iCre+* referred to as *Ube2i* conditional knockout (cKO).

Tissue collection, histological analysis and follicle quantification

Mice were anesthetized by isoflurane (Abbott Laboratories) inhalation and euthanized by cervical dislocation. Ovaries were collected at multiple time points and fixed in 10% neutral buffered formalin (Electron Microscopy Services) overnight followed by standard paraffin processing and embedding at the Human Tissue Acquisition and Pathology Core at Baylor College of Medicine. A minimum of four ovaries for each genotype and time point were serially sectioned (5 µm thick) and stained with periodic acid-Schiff for morphometric analysis. High-resolution images were obtained using a Mikroscan D2 digital slide scanner (Meyer Instruments) or a digital camera (AxioCam 105; Zeiss) at 100× magnification. For morphogenetics, follicles in every fifth section were counted manually; to avoid double counting, only follicles with a visible oocyte nucleus were counted. A correction factor for follicles smaller than the antral stage was applied to all samples uniformly (Tilly, 2003). Antral follicles and CL were counted in full by following follicles individually through serial images. Follicles were classified into the following categories based on previous studies (Pedersen and Peters, 1968): primordial (type 2), primary (types 3a and 3b), secondary (type 4), preantral (types 5a and 5b) and antral (types 6 to 8). Atretic follicles were classified based on discontinuous basement membrane, collapsed zona pellucida, pyknotic nuclei in granulosa cells, shrunken oocytes, and irregular follicle size.

Fertility analysis

Mating pairs of a *Ube2i* cKO female or control littermate and a known fertile wild-type male were housed in a continuous breeding cage after reaching sexual maturity (6-8 weeks of age). The presence of newborn pups was monitored daily for 6 months and resulting litters were weaned at 3 weeks. The numbers of pups per litter and litters per month were recorded for five females per genotype.

Hormone analysis

Blood was retrieved from isoflurane-anesthetized 8-week-old mice by cardiac puncture, and serum was separated by centrifugation (15,777 ***g*** for 5 min) in microtainer collection tubes (Becton, Dickinson and Company) and frozen at −20°C until assayed. Mouse FSH and AMH levels were analyzed by ELISA at the University of Virginia Ligand Core Facility (Specialized Cooperative Centers Program in Reproductive Research NICHD/NIH U54-HD28934). Assay method information is available online. The Ligand Core uses the Millipore Pituitary Panel Multiplex kit (MPTMAG-49K) to measure FSH in mouse serum samples and the Ansh (rat and mouse) ELISA for AMH determination (AL-113, Ansh Labs). Data were log transformed before statistical analysis by Student's *t*-test, but are presented in figures as concentrations.

Development (2019) 146, dev176701. doi:10.1242/dev.176701

Superovulation and *in vitro* maturation of oocytes

For superovulation, 3-week-old female mice were injected intraperitoneally with 5 IU eCG (VWR), and 47 h later, injected intraperitoneally with 5 IU hCG (Pregnyl; Merck Pharmaceuticals). Mice were euthanized 17-18 h after the hCG injection and oocytes harvested from the oviduct ampulla. For *in vitro* maturation, mice were injected intraperitoneally with 5 IU eCG and euthanized 46-48 h post-injection. Oocytes were released from follicles using a 26.5 gauge needle and collected into M2 medium containing 2.5 µM milrinone (Sigma-Aldrich) to maintain meiotic arrest (Tsafriri et al., 1996). Prior to oocyte collection, EmbryoSlides (Vitrolife) were preconditioned by placing CZB medium (Millipore Sigma) supplemented with 2 mM L-glutamine (Thermo Fisher Scientific) in the wells, which were then covered with a thin layer of mineral oil, and incubated at 37°C in 5% CO_2 overnight. After being denuded, oocytes were rinsed in milrinone-free M2 medium and one to three oocytes were transferred to each preconditioned well. Slides were incubated in an EmbryoScope Time-Lapse System (Vitrolife) for 24 h with images obtained every 10-20 min. The percentage of oocytes that underwent GVBD and extruded polar bodies was determined for each experimental group. Statistical analysis was performed on raw data.

Immunofluorescence and immunohistochemistry

Paraffin-embedded sections were deparaffinized, rehydrated, and boiled in citrate buffer for antigen retrieval as previously described (Pangas et al., 2006; Rajkovic et al., 2004). Non-specific signal was blocked with 3% bovine serum albumin (BSA, Invitrogen) in Tris-buffered saline 0.1% Tween (TBS-T) for 1 h, and slides were incubated overnight at 4°C in a humidified chamber with primary antibodies specific to NOBOX (1:1000; goat anti-NOBOX) (Rajkovic et al., 2004) and UBE2I (1:250; rabbit anti-UBE2i/UBC9; Abcam Ab33044). After TBS-T washes, slides were incubated with biotinylated (1:200; Vector Laboratories, BA-9500) or Alexa Fluor 488-conjugated (1:200; Life Technologies, A21206) antibody for 1 h at room temperature. For immunofluorescence staining, sections were washed in TBS-T, incubated with 4′,6-diamidino-2-phenylindole (DAPI) (1:1000; Sigma-Aldrich), and mounted with VECTASHIELD medium (Vector Laboratories). For immunohistochemistry staining, sections were incubated with VECTASTAIN ABC solution (Vector Laboratories), and, subsequently, with 3,3′-diaminobenzidine (DAB) substrate (Vector Laboratories) for peroxidase-based detection of immunoreactive signals. Sections were counterstained with Harris Hematoxylin (Sigma-Aldrich), dehydrated using an alcohol gradient, and mounted with Permount (Fisher Scientific). For immunofluorescence staining of ovulated oocytes, oocytes were collected from the oviduct ampulla of superovulated mice into M2 medium (Sigma-Aldrich) with 0.3 mg/ml hyaluronidase (Sigma-Aldrich), denuded by pipetting, and fixed in 2.5% paraformaldehyde (PFA) (Thermo Fisher Scientific) in PBS for 20 min followed by permeabilization in 0.01% Triton X-100 (Thermo Fisher Scientific) in PBS for 15 min. Antigen blocking was performed in 1% BSA in PBS-T for 15 min and then incubated in alpha-tubulin monoclonal antibody (clone B-5-1-2) conjugated to Alexa Fluor 488 (1:100; Thermo Fisher Scientific, 322588) diluted in blocking buffer for 1 h at room temperature, followed by three 5-min washes in blocking buffer. Chromosomes were labeled by DAPI staining in PBS (1 µg/ml) for 5 min and then washed once in PBS. Stained oocytes were mounted in VECTASHIELD hardset mounting medium (Vector Laboratories), allowed to dry, and sealed with nail polish.

RNA isolation and qPCR

For total RNA isolation, mouse ovaries were harvested and stored in RNAlater (Life Technologies). Total RNA was extracted using the RNeasy Micro kit (Qiagen) and DNased prior to cDNA generation or primers were designed to span an intron. For RNA isolation from oocytes, GV-stage oocytes were collected from eCG-stimulated mice and total RNA extracted using the Arcturus PicoPure RNA Isolation Kit (Thermo Fisher Scientific). cDNA was synthesized from 200 ng of total RNA with the High-Capacity RNA-to-cDNA reverse transcription kit (Life Technologies). Real-time quantitative PCR (qPCR) assays were carried out with Fast SYBR Green Master Mix (Life Technologies) according to the manufacturer's protocol. Melt curve analysis was performed to verify a single amplification peak. qPCR primer sequences (Table S3) were designed using PrimerBank (https://pga.mgh.harvard.edu/primerbank/) and purchased from Integrated DNA Technologies. The relative mRNA levels of transcript were calculated by the cycle threshold ($2^{-\Delta\Delta CT}$) method (Livak and Schmittgen, 2001). *Gapdh* or *Rpl19* was used as a reference gene to normalize RNA, and the data are shown relative to the mean of the control samples.

RNA-sequencing analysis

For RNA sequencing, one ovary each from three *Ube2i*$^{loxP/loxP}$ control or three *Ube2i* cKO mice were pooled per biological replicate (n=3 pools of 3 ovaries per genotype) with the same amount of total RNA. Sample quality analysis was performed at Genomic and RNA Profiling Core (GARP) at Baylor College of Medicine. RNA sequencing was performed on an Illumina HiSeq 2500 system by the GARP at Baylor College of Medicine. Paired-end sequencing (100 bp reads) was implemented for all samples to permit more accurate read alignment and improve sequencing efficiency. Reads were mapped to the mouse genome build UCSC mm10 (NCBI 38) using TopHat2 (Kim et al., 2013; Trapnell et al., 2010) and gene expression (in fragments per kilobase of exon model per million reads mapped, FPKM) was assessed using Cufflinks2 (Trapnell et al., 2010). Combined data were quantile normalized using the R statistical system. Significantly differentiated genes between control and *Ube2i* cKO mice were identified using a parametric *t*-test with P<0.05 and fold change of at least 1.5. IPA was performed on the *Ube2i* cKO signature to assess enriched upstream regulators. GO analysis of DEGs was performed using DAVID v6.8 (https://david.ncifcrf.gov/) (Huang et al., 2009a,b). IPA (Qiagen) was performed at Baylor College of Medicine. RNA-seq data have been deposited in the NCBI's Gene Expression Omnibus database (accession number GSE133179).

Cell lines and reagents

HEK-293T cells were purchased from ATCC and cultured in Dulbecco's modified Eagle's medium (Invitrogen) supplemented with 10% fetal bovine serum. Expression plasmids for MYC-SUMO1ρ and MYC-SUMO2ρ, which are mostly resistant to deSUMOylation, were kindly provided by Dr Deborah Johnson (Baylor College of Medicine). Full-length FLAG-tagged mouse *Nobox* was cloned into pCMV-Tag2A and verified by DNA sequencing. HEK-293T cells were grown to 50% confluence, then transfected with JetPrime reagent following the manufacturer's recommendations. Cells were grown for 48 h then harvested in 1 ml of Mammalian Protein Extraction Reagent (M-PER) (Thermo Fisher Scientific) with protease inhibitor cocktail for general use (Sigma-Aldrich).

Immunoblotting

Ovaries from 2-week-old mice were collected and homogenized in 50 µl T-PER tissue protein extraction reagent (Thermo Fisher Scientific) with EDTA-free protease inhibitor (Sigma-Aldrich). Samples were prepared by loading 10 µl of total protein with LDS sample buffer (Invitrogen) and sample reducing agent (Invitrogen), then incubated at 70°C for 10 min. Samples were cooled to room temperature and loaded into NuPAGE 4-12% bis-tris protein gels (Invitrogen) and run at 200 V for 50 min in MOPS SDS running buffer (Invitrogen) under reducing conditions. Proteins were transferred to nitrocellulose membranes (Thermo Fisher Scientific) in NuPAGE transfer buffer (Invitrogen) with 10% methanol (VWR) at 30 V for 1 h. After transfer, membranes were allowed to dry. Non-specific antigen blocking was carried out by incubating membranes in 5% non-fat milk in TBS-T for at least 2 h. Primary antibodies (goat anti-NOBOX, 1:2000; a gift from Dr Aleksander Rajkovic, University of California, San Francisco, USA; mouse anti-β-actin clone C4 sc-47778, 1:2000, Santa Cruz Biotechnology) were diluted in 3% milk in TBS-T and incubated on membranes with rocking at 4°C overnight. Membranes were rinsed once with TBS-T followed by a 15-min TBS-T wash and two 5-min TBS-T washes. Secondary antibodies (HRP-conjugated donkey anti-goat IgG, 1:15,000, Jackson ImmunoResearch Laboratories, 705-035-147; HRP-conjugated donkey anti-mouse IgG, 1:15,000, Vector Laboratories, 715-035-150) were diluted in 3% milk in TBS-T and incubated on the membrane for 1 h at room temperature with rocking, and then washed in TBS-T as described above. Chemiluminescent detection was performed with SuperSignal West Pico PLUS chemiluminescent substrate (Thermo Fisher Scientific) or Pierce

ECL western blotting substrate (Thermo Fisher Scientific) according to the manufacturer's directions. Signal detection was performed on HyBlot CL autoradiography film (Thomas Scientific) developed using a Konica SRX-101A medical film processor (Konica Minolta Medical and Graphic). Quantification was carried out using ImageJ software and statistical analysis was performed on normalized data by unpaired Student's *t*-test.

Immunoprecipitation

Cell lysate (1.4 mg) was immunoprecipitated using 40 µl of anti-FLAG-M2 beads (Sigma-Aldrich). The lysate/bead mixture was incubated overnight at 4°C. Beads were washed three times in TBS and eluted in 100 µl of 1× LDS sample buffer with β-mercaptoethanol. For input lanes, 20 µg of protein was loaded with 1× LDS sample buffer (Invitrogen) and sample reducing reagent (Invitrogen) and processed as above. Rabbit anti-Myc-Tag (1:1000; Cell Signaling Technology, 2278) was used for the primary antibody and anti-rabbit HRP (1:20,000; Jackson ImmunoResearch, 711-035-152) used as the secondary antibody. The membrane was stripped for 15 min in stripping buffer (Thermo Fisher Scientific) and re-probed using rabbit-anti-FLAG (F7425, Sigma-Aldrich) at 1:5000 and the same anti-rabbit secondary at 1:20,000.

Statistical analysis

All experiments were performed with at least three independent replicates. GraphPad Prism 8 was used for statistical analysis. The number of replicates or numbers of mice are indicated in the figure legends. Fertility data, ovarian weights, qPCR and immunoblot quantification are shown as mean and s.e.m. The difference between two groups was determined by Student's *t*-test and differences between multiple groups by ANOVA followed by post-hoc testing. ELISA data were log-transformed prior to statistical analysis by Student's *t*-test. All *t*-tests were two-tailed. For meiotic resumption, Fisher's Exact test was performed on raw data. $P<0.05$ was considered statistically significant.

Acknowledgements

The authors wish to thank members of the Genomic and RNA Profiling Core, Genetically Engineered Mouse Core, Pathology and Histology Core, and Embryonic Stem Cell core at Baylor College of Medicine for their assistance with these studies. We thank Dr Robert T. Rydze with assistance with statistical analysis, manuscript editing, and figure preparation for previous drafts. We thank Dr Diana Monsivais for technical advice and Alyssa Alaniz for assistance with RNA sequencing and database analysis. We thank Austin Cooney for providing the *Gdf9iCre*+ mouse model. We thank Dr Deborah L. Johnson (BCM) for the *Myc-Sumo1ρ* and *Myc-Sumo2ρ* expression plasmids. The authors also acknowledge the University of Virginia Ligand Assay and Analysis Core for aiding the serum studies. Core services at Baylor College of Medicine were supported with funding from the NIH (NCI grant P30 CA125123 and NIEHS grant P30 ES030285).

Competing interests

The authors declare no competing or financial interests.

Author contributions

Conceptualization: A. Rodriguez, S.M.B., S.K.T., S.A.P.; Validation: S.K.T.; Formal analysis: A. Rodriguez, S.M.B., B.K.P., K.R., C.C., S.A.P.; Resources: A. Rajkovic, A.A., A.D.; Writing - original draft: A. Rodriguez, S.A.P.; Writing - review & editing: S.M.B., B.K.P., S.K.T., S.A.P.; Supervision: S.A.P.; Project administration: S.A.P.; Funding acquisition: S.A.P.

Funding

This work was supported by the National Institutes of Health (CA125123, HD028934, HD085994 to S.A.P.) and the Ligue Nationale Contre le Cancer (LNCC) (A.D.). Deposited in PMC for release after 12 months.

Data availability

RNA-sequencing files have been deposited in Gene Expression Omnibus under accession number GSE133179.

Supplementary information

Supplementary information available online at
http://dev.biologists.org/lookup/doi/10.1242/dev.176701.supplemental

References

Ballow, D. J., Xin, Y., Choi, Y., Pangas, S. A. and Rajkovic, A. (2006). Sohlh2 is a germ cell-specific bHLH transcription factor. *Gene Expr. Patterns* **6**, 1014-1018. doi:10.1016/j.modgep.2006.04.007

Békés, M., Prudden, J., Srikumar, T., Raught, B., Boddy, M. N. and Salvesen, G. S. (2011). The dynamics and mechanism of SUMO chain deconjugation by SUMO-specific proteases. *J. Biol. Chem.* **286**, 10238-10247. doi:10.1074/jbc.M110.205153

Belli, M., Cimadomo, D., Merico, V., Redi, C. A., Garagna, S. and Zuccotti, M. (2013). The NOBOX protein becomes undetectable in developmentally competent antral and ovulated oocytes. *Int. J. Dev. Biol.* **57**, 35-39. doi:10.1387/ijdb.120125mz

Bouilly, J., Bachelot, A., Broutin, I., Touraine, P. and Binart, N. (2011). Novel NOBOX loss-of-function mutations account for 6.2% of cases in a large primary ovarian insufficiency cohort. *Hum. Mutat.* **32**, 1108-1113. doi:10.1002/humu.21543

Bouilly, J., Roucher-Boulez, F., Gompel, A., Bry-Gauillard, H., Azibi, K., Beldjord, C., Dodé, C., Bouligand, J., Mantel, A. G., Hécart, A.-C. et al. (2015). New NOBOX mutations identified in a large cohort of women with primary ovarian insufficiency decrease KIT-L expression. *J. Clin. Endocrinol. Metab.* **100**, 994-1001. doi:10.1210/jc.2014-2761

Briley, S. M., Jasti, S., McCracken, J. M., Hornick, J. E., Fegley, B., Pritchard, M. T. and Duncan, F. E. (2016). Reproductive age-associated fibrosis in the stroma of the mammalian ovary. *Reproduction* **152**, 245-260. doi:10.1530/REP-16-0129

Choi, Y., Yuan, D. and Rajkovic, A. (2008). Germ cell-specific transcriptional regulator sohlh2 is essential for early mouse folliculogenesis and oocyte-specific gene expression. *Biol. Reprod.* **79**, 1176-1182. doi:10.1095/biolreprod.108.071217

Dewailly, D., Andersen, C. Y., Balen, A., Broekmans, F., Dilaver, N., Fanchin, R., Griesinger, G., Kelsey, T. W., La Marca, A., Lambalk, C. et al. (2014). The physiology and clinical utility of anti-Müllerian hormone in women. *Hum. Reprod. Update* **20**, 370-385. doi:10.1093/humupd/dmt062

Ding, Y., Kaido, M., Llano, E., Pendas, A. M. and Kitajima, T. S. (2018). The post-anaphase SUMO pathway ensures the maintenance of centromeric cohesion through meiosis I-II transition in mammalian oocytes. *Curr. Biol.* **28**, 1661-1669.e1664. doi:10.1016/j.cub.2018.04.019

Dokshin, G. A., Baltus, A. E., Eppig, J. J. and Page, D. C. (2013). Oocyte differentiation is genetically dissociable from meiosis in mice. *Nat. Genet.* **45**, 877-883. doi:10.1038/ng.2672

Dong, J., Albertini, D. F., Nishimori, K., Kumar, T. R., Lu, N. and Matzuk, M. M. (1996). Growth differentiation factor-9 is required during early ovarian folliculogenesis. *Nature* **383**, 531-535. doi:10.1038/383531a0

Elvin, J. A., Clark, A. T., Wang, P., Wolfman, N. M. and Matzuk, M. M. (1999). Paracrine actions of growth differentiation factor-9 in the mammalian ovary. *Mol. Endocrinol.* **13**, 1035-1048. doi:10.1210/mend.13.6.0310

Feitosa, W. B. and Morris, P. L. (2018). SUMOylation regulates germinal vesicle breakdown and the Akt/PKB pathway during mouse oocyte maturation. *Am. J. Physiol. Cell Physiol.* **315**, C115-C121. doi:10.1152/ajpcell.00038.2018

Geiss-Friedlander, R. and Melchior, F. (2007). Concepts in sumoylation: a decade on. *Nat. Rev. Mol. Cell Biol.* **8**, 947-956. doi:10.1038/nrm2293

Hay, R. T. (2005). SUMO: a history of modification. *Mol. Cell* **18**, 1-12. doi:10.1016/j.molcel.2005.03.012

Hilgarth, R. S., Murphy, L. A., Skaggs, H. S., Wilkerson, D. C., Xing, H. and Sarge, K. D. (2004). Regulation and function of SUMO modification. *J. Biol. Chem.* **279**, 53899-53902. doi:10.1074/jbc.R400021200

Huang, D. W., Sherman, B. T. and Lempicki, R. A. (2009a). Bioinformatics enrichment tools: paths toward the comprehensive functional analysis of large gene lists. *Nucleic Acids Res.* **37**, 1-13. doi:10.1093/nar/gkn923

Huang, D. W., Sherman, B. T. and Lempicki, R. A. (2009b). Systematic and integrative analysis of large gene lists using DAVID bioinformatics resources. *Nat. Protoc.* **4**, 44-57. doi:10.1038/nprot.2008.211

Ihara, M., Stein, P. and Schultz, R. M. (2008). UBE2I (UBC9), a SUMO-conjugating enzyme, localizes to nuclear speckles and stimulates transcription in mouse oocytes. *Biol. Reprod.* **79**, 906-913. doi:10.1095/biolreprod.108.070474

Johnson, E. S. (2004). Protein modification by SUMO. *Annu. Rev. Biochem.* **73**, 355-382. doi:10.1146/annurev.biochem.73.011303.074118

Jolly, A., Bayram, Y., Turan, S., Aycan, Z., Tos, T., Abali, Z. Y., Hacihamdioglu, B., Coban Akdemir, Z. H., Hijazi, H., Bas, S. et al. (2019). Exome sequencing of a primary ovarian insufficiency cohort reveals common molecular etiologies for a spectrum of disease. *J. Clin. Endocrinol. Metab.* **104**, 3049-3067. doi:10.1210/jc.2019-00248

Kevenaar, M. E., Meerasahib, M. F., Kramer, P., van de Lang-Born, B. M. N., de Jong, F. H., Groome, N. P., Themmen, A. P. N. and Visser, J. A. (2006). Serum anti-müllerian hormone levels reflect the size of the primordial follicle pool in mice. *Endocrinology* **147**, 3228-3234. doi:10.1210/en.2005-1588

Kim, D., Pertea, G., Trapnell, C., Pimentel, H., Kelley, R. and Salzberg, S. L. (2013). TopHat2: accurate alignment of transcriptomes in the presence of insertions, deletions and gene fusions. *Genome Biol.* **14**, R36. doi:10.1186/gb-2013-14-4-r36

Kumar, R., Alwani, M., Kosta, S., Kaur, R. and Agarwal, S. (2017). BMP15 and GDF9 gene mutations in premature ovarian failure. *J Reprod Infertil* **18**, 185-189.
Lan, Z.-J., Xu, X. and Cooney, A. J. (2004). Differential oocyte-specific expression of Cre recombinase activity in GDF-9-iCre, Zp3cre, and Msx2Cre transgenic mice. *Biol. Reprod.* **71**, 1469-1474. doi:10.1095/biolreprod.104.031757
Lechowska, A., Bilinski, S., Choi, Y., Shin, Y., Kloc, M. and Rajkovic, A. (2011). Premature ovarian failure in nobox-deficient mice is caused by defects in somatic cell invasion and germ cell cyst breakdown. *J. Assist. Reprod. Genet.* **28**, 583-589. doi:10.1007/s10815-011-9553-5
Liang, L., Soyal, S. M. and Dean, J. (1997). FIGalpha, a germ cell specific transcription factor involved in the coordinate expression of the zona pellucida genes. *Development* **124**, 4939-4947.
Livak, K. J. and Schmittgen, T. D. (2001). Analysis of relative gene expression data using real-time quantitative PCR and the 2−ΔΔCT Method. *Methods* **25**, 402-408. doi:10.1006/meth.2001.1262
Munsterberg, A. and Lovell-Badge, R. (1991). Expression of the mouse anti-mullerian hormone gene suggests a role in both male and female sexual differentiation. *Development* **113**, 613-624.
Nacerddine, K., Lehembre, F., Bhaumik, M., Artus, J., Cohen-Tannoudji, M., Babinet, C., Pandolfi, P. P. and Dejean, A. (2005). The SUMO pathway is essential for nuclear integrity and chromosome segregation in mice. *Dev. Cell* **9**, 769-779. doi:10.1016/j.devcel.2005.10.007
Nelson, L. M. (2009). Clinical practice. Primary ovarian insufficiency. *N. Engl. J. Med.* **360**, 606-614. doi:10.1056/NEJMcp0808697
Nie, M., Xie, Y., Loo, J. A. and Courey, A. J. (2009). Genetic and proteomic evidence for roles of Drosophila SUMO in cell cycle control, Ras signaling, and early pattern formation. *PLoS ONE* **4**, e5905. doi:10.1371/journal.pone.0005905
Oh, S. R., Choe, S. Y. and Cho, Y. J. (2019). Clinical application of serum anti-Müllerian hormone in women. *Clin. Exp. Reprod Med.* **46**, 50-59. doi:10.5653/cerm.2019.46.2.50
Pangas, S. A., Choi, Y., Ballow, D. J., Zhao, Y., Westphal, H., Matzuk, M. M. and Rajkovic, A. (2006). Oogenesis requires germ cell-specific transcriptional regulators Sohlh1 and Lhx8. *Proc. Natl. Acad. Sci. USA* **103**, 8090-8095. doi:10.1073/pnas.0601083103
Pedersen, T. and Peters, H. (1968). Proposal for a classification of oocytes and follicles in the mouse ovary. *J. Reprod. Fertil.* **17**, 555-557. doi:10.1530/jrf.0.0170555
Pelisch, F., Tammsalu, T., Wang, B., Jaffray, E. G., Gartner, A. and Hay, R. T. (2017). A SUMO-dependent protein network regulates chromosome congression during oocyte meiosis. *Mol. Cell* **65**, 66-77. doi:10.1016/j.molcel.2016.11.001
Pelisch, F., Bel Borja, L., Jaffray, E. G. and Hay, R. T. (2019). Sumoylation regulates protein dynamics during meiotic chromosome segregation in C. elegans oocytes. *J. Cell Sci.* **132**, jcs232330. doi:10.1242/jcs.232330.
Pelosi, E., Simonsick, E., Forabosco, A., Garcia-Ortiz, J. E. and Schlessinger, D. (2015). Dynamics of the ovarian reserve and impact of genetic and epidemiological factors on age of menopause. *Biol. Reprod.* **92**, 130. doi:10.1095/biolreprod.114.127381
Peng, J., Li, Q., Wigglesworth, K., Rangarajan, A., Kattamuri, C., Peterson, R. T., Eppig, J. J., Thompson, T. B. and Matzuk, M. M. (2013). Growth differentiation factor 9:bone morphogenetic protein 15 heterodimers are potent regulators of ovarian functions. *Proc. Natl. Acad. Sci. USA* **110**, E776-E785. doi:10.1073/pnas.1218020110
Qiao, H., Rao, H. B. D. P., Yun, Y., Sandhu, S., Fong, J. H., Sapre, M., Nguyen, M., Tham, A., Van, B. W., Chng, T. Y. H. et al. (2018). Impeding DNA break repair enables oocyte quality control. *Mol. Cell* **72**, 211-221.e213. doi:10.1016/j.molcel.2018.08.031
Qin, Y., Choi, Y., Zhao, H., Simpson, J. L., Chen, Z.-J. and Rajkovic, A. (2007). NOBOX homeobox mutation causes premature ovarian failure. *Am. J. Hum. Genet.* **81**, 576-581. doi:10.1086/519496
Rajkovic, A., Pangas, S. A., Ballow, D., Suzumori, N. and Matzuk, M. M. (2004). NOBOX deficiency disrupts early folliculogenesis and oocyte-specific gene expression. *Science* **305**, 1157-1159. doi:10.1126/science.1099755
Rohira, A. D., Chen, C.-Y., Allen, J. R. and Johnson, D. L. (2013). Covalent small ubiquitin-like modifier (SUMO) modification of Maf1 protein controls RNA polymerase III-dependent transcription repression. *J. Biol. Chem.* **288**, 19288-19295. doi:10.1074/jbc.M113.473744
Rosonina, E., Akhter, A., Dou, Y., Babu, J. and Sri Theivakadadcham, V. S. (2017). Regulation of transcription factors by sumoylation. *Transcription* **8**, 220-231. doi:10.1080/21541264.2017.1311829
Salmon, N. A., Handyside, A. H. and Joyce, I. M. (2004). Oocyte regulation of anti-Müllerian hormone expression in granulosa cells during ovarian follicle development in mice. *Dev. Biol.* **266**, 201-208. doi:10.1016/j.ydbio.2003.10.009
Shin, Y.-H., Ren, Y., Suzuki, H., Golnoski, K. J., Ahn, H. W., Mico, V. and Rajkovic, A. (2017). Transcription factors SOHLH1 and SOHLH2 coordinate oocyte differentiation without affecting meiosis I. *J. Clin. Invest.* **127**, 2106-2117. doi:10.1172/JCI90281
Soyal, S. M., Amleh, A. and Dean, J. (2000). FIGalpha, a germ cell-specific transcription factor required for ovarian follicle formation. *Development* **127**, 4645-4654.
Su, Y.-Q., Wu, X., O'Brien, M. J., Pendola, F. L., Denegre, J. N., Matzuk, M. M. and Eppig, J. J. (2004). Synergistic roles of BMP15 and GDF9 in the development and function of the oocyte-cumulus cell complex in mice: genetic evidence for an oocyte-granulosa cell regulatory loop. *Dev. Biol.* **276**, 64-73. doi:10.1016/j.ydbio.2004.08.020
Su, Y.-Q., Sugiura, K., Wigglesworth, K., O'Brien, M. J., Affourtit, J. P., Pangas, S. A., Matzuk, M. M. and Eppig, J. J. (2008). Oocyte regulation of metabolic cooperativity between mouse cumulus cells and oocytes: BMP15 and GDF9 control cholesterol biosynthesis in cumulus cells. *Development* **135**, 111-121. doi:10.1242/dev.009068
Sun, W., Stegmann, B. J., Henne, M., Catherino, W. H. and Segars, J. H. (2008). A new approach to ovarian reserve testing. *Fertil. Steril.* **90**, 2196-2202. doi:10.1016/j.fertnstert.2007.10.080
Suzumori, N., Yan, C., Matzuk, M. M. and Rajkovic, A. (2002). Nobox is a homeobox-encoding gene preferentially expressed in primordial and growing oocytes. *Mech. Dev.* **111**, 137-141. doi:10.1016/S0925-4773(01)00620-7
Suzumori, N., Pangas, S. A. and Rajkovic, A. (2007). Candidate genes for premature ovarian failure. *Curr. Med. Chem.* **14**, 353-357. doi:10.2174/092986707779941087
Tilly, J. L. (2003). Ovarian follicle counts–not as simple as 1, 2, 3. *Reprod. Biol. Endocrinol.* **1**, 11. doi:10.1186/1477-7827-1-11
Trapnell, C., Williams, B. A., Pertea, G., Mortazavi, A., Kwan, G., van Baren, M. J., Salzberg, S. L., Wold, B. J. and Pachter, L. (2010). Transcript assembly and quantification by RNA-Seq reveals unannotated transcripts and isoform switching during cell differentiation. *Nat. Biotechnol.* **28**, 511-515. doi:10.1038/nbt.1621
Tsafriri, A., Chun, S.-Y., Zhang, R., Hsueh, A. J. W. and Conti, M. (1996). Oocyte maturation involves compartmentalization and opposing changes of cAMP levels in follicular somatic and germ cells: studies using selective phosphodiesterase inhibitors. *Dev. Biol.* **178**, 393-402. doi:10.1006/dbio.1996.0226
Ulrich, H. D. (2008). The fast-growing business of SUMO chains. *Mol. Cell* **32**, 301-305. doi:10.1016/j.molcel.2008.10.010
van Houten, E. L. A. F., Themmen, A. P. N. and Visser, J. A. (2010). Anti-Müllerian hormone (AMH): regulator and marker of ovarian function. *Ann. Endocrinol.* **71**, 191-197. doi:10.1016/j.ando.2010.02.016
Verger, A., Perdomo, J. and Crossley, M. (2003). Modification with SUMO. A role in transcriptional regulation. *EMBO Rep.* **4**, 137-142. doi:10.1038/sj.embor.embor738
Visser, J. A., Schipper, I., Laven, J. S. E. and Themmen, A. P. N. (2012). Anti-Müllerian hormone: an ovarian reserve marker in primary ovarian insufficiency. *Nat. Rev. Endocrinol.* **8**, 331-341. doi:10.1038/nrendo.2011.224
Wang, Z.-B., Ou, X.-H., Tong, J.-S., Li, S., Wei, L., Ouyang, Y.-C., Hou, Y., Schatten, H. and Sun, Q.-Y. (2010). The SUMO pathway functions in mouse oocyte maturation. *Cell Cycle* **9**, 2640-2646. doi:10.4161/cc.9.13.12120
Yan, C., Wang, P., DeMayo, J., DeMayo, F. J., Elvin, J. A., Carino, C., Prasad, S. V., Skinner, S. S., Dunbar, B. S., Dube, J. L. et al. (2001). Synergistic roles of bone morphogenetic protein 15 and growth differentiation factor 9 in ovarian function. *Mol. Endocrinol.* **15**, 854-866. doi:10.1210/mend.15.6.0662
Yuan, Y.-F., Zhai, R., Liu, X.-M., Khan, H. A., Zhen, Y.-H. and Huo, L.-J. (2014). SUMO-1 plays crucial roles for spindle organization, chromosome congression, and chromosome segregation during mouse oocyte meiotic maturation. *Mol. Reprod. Dev.* **81**, 712-724. doi:10.1002/mrd.22339
Zhao, H., Qin, Y., Kovanci, E., Simpson, J. L., Chen, Z.-J. and Rajkovic, A. (2007). Analyses of GDF9 mutation in 100 Chinese women with premature ovarian failure. *Fertil. Steril.* **88**, 1474-1476. doi:10.1016/j.fertnstert.2007.01.021
Zhao, Q., Xie, Y., Zheng, Y., Jiang, S., Liu, W., Mu, W., Liu, Z., Zhao, Y., Xue, Y. and Ren, J. (2014). GPS-SUMO: a tool for the prediction of sumoylation sites and SUMO-interaction motifs. *Nucleic Acids Res.* **42**, W325-W330. doi:10.1093/nar/gku383
Zhu, J.-L., Lin, S.-L., Li, M., Ouyang, Y.-C., Hou, Y., Schatten, H. and Sun, Q.-Y. (2010). Septin2 is modified by SUMOylation and required for chromosome congression in mouse oocytes. *Cell Cycle* **9**, 1607-1616. doi:10.4161/cc.9.8.11463